TAO, Vol. 9, No. 2, 239-254, June 1998

The Solar Wind Control of the Magnetopause Shape : A Comparison of A Model Magnetopause and Empirical Models

Ching-Chang Cheng[1]

(Manuscript received 8 January 1997, in final form 12 April 1998)

ABSTRACT

The solar wind control of the magnetopause shape is studied with a model magnetopause that results from three sources of magnetic field. One source is the geomagnetic field produced by the Earth's dipole. Another results from an image dipole placed in front of the magnetopause to produce the effect of the magnetopause current which limits the spatial extent of the geomagnetic field. The third is a southward interplanetary magnetic field (IMF) in the Earth's vicinity. With an image dipole strength and the location to account for the effect of the solar wind dynamic pressure (D_p), the shape of the model magnetopause can be regarded as controlled by D_p and the southward IMF. As an image dipole strength is about fourteen times the Earth's dipole and the location is at thirty times the Earth's radius, the shape of the model magnetopause is consistent with observational results for a southward IMF. A comparison of the shape of the model magnetopause and an empirical model by Shue *et al.* (1997) shows that the image dipole strength at a fixed location correlates linearly with D_p for a southward IMF. In addition, they agree qualitatively for high D_p and a southward IMF.

(Key words: Solar wind, Magnetopause, IMF)

1. INTRODUCTION

The Earth's magnetosphere has generally been thought to be determined by the solar wind, the interplanetary magnetic field (IMF), and the geomagnetic field. Magnetospheric configuration is widely considered a useful means to describe the global picture of the Earth's magnetosphere. It is also conducive to understanding physical mechanisms of the formation of the Earth's magnetosphere (e.g. Nishida, 1978). In the past, there were two main models of magnetospheric configuration to describe the Earth's magnetosphere. From the balance between the dynamic pressure of the impinging solar wind and the magnetic pressure of the geomagnetic field, Chapman and Ferraro (1931) suggested that the magnetosphere might be

[1]Institute of Space Science, National Central University, Chung-Li, and Department of Physics, National Hu-Wei Institute of Technology, Hu-Wei, Taiwan, R.O.C.

closed. In order to study the cause of magnetospheric convection, Dungey (1961) proposed an open model of the magnetosphere in which the Earth's dipole is permeated by a southward IMF. Based on these two models of the magnetosphere, many studies have been conducted to explain various local magnetospheric phenomena.

In recent years, the spacecraft and satellites launched to probe the Earth's environment have collected valuable data from which some features of the magnetosphere are revealed. High-latitude HEOS 2 measurements near the dayside magnetopause showed that the magnetic field converges toward a cusp which presumably results from Chapman-Ferraro currents (Fairfield, 1977; Haerendel *et al.*, 1978). On the night side, geomagnetic field lines are interconnected with the interplanetary space (Fairfield, 1987 and references therein). The observational evidence indicates that both the convergence of the magnetic field toward the cusp and the penetration of the IMF may take place jointly. In other words, the magnetosphere could be partially closed and partially open. Thus, it is useful to construct a theoretical model to exhibit some of these features of the magnetosphere.

The terrestrial magnetopause is generally identified as the surface of separation between the geomagnetic field and the IMF. It has long been known that the shape of the magnetopause is mainly controlled by the solar wind dynamic pressure D_p and the IMF B_z component (see review by Fairfield, 1995). Recently, with the availability of large numbers of magnetopause crossings, the magnetopause shape has been fitted as a function of D_p and the IMF B_z component (Sibeck *et al.*, 1991; Petrinec *et al.*, 1991; Roelof and Sibeck, 1993; Petrinec and Russell, 1993; Shue *et al.*, 1997). Due to the limit of the functional form or satellite orbits, some empirical models are appropriate for the dayside region (e.g. Roelof and Sibeck, 1993) and some for the nightside region (e.g. Petrinec and Russell, 1993). Nevertheless, a common trend in these studies exists whereby increased pressure compresses the magnetopause earthward while IMF B_z remains steady. Moreover, the flank expands with increasing IMF B_z and the subsolar distance reduces conspicuously at low D_p and less at high D_p. Thus, comparison of a model magnetopause with empirical models helps in realizing how the magnetopause shape is controlled by the solar wind.

Recently, Yeh (1997) proposed a mathematical model to study magnetospheric structure with a southward IMF. In the model, the IMF is assumed to be due south and moderate as its magnitude is less than the geomagnetic field at the subsolar point. The model magnetosphere possesses features of both a closed model and an open model, as revealed by observations. Since the realistic magnetopause shape is more affected by IMF B_z than other components such as B_x and B_y, it seems appropriate that a model magnetopause for a southward IMF can be used to study how the magnetopause shape is controlled by the solar wind. Hence, the main goal of this study is to examine qualitatively the solar wind control of the magnetopause shape by comparing a model magnetopause based on Yeh (1997) with empirical models. This paper is organized as follows. Section 2 mathematically shows that a model magnetopause is constructed on three magnetic fields. Section 3 discusses the shape of the model magnetopause and compare it with empirical models. Finally, the last section discusses other factors affecting the comparison of the model magnetopause and empirical models, and summarizes this study.

2. A MODEL MAGNETOPAUSE FOR THE SOUTHWARD IMF

Referring to Yeh (1997), a mathematical model of the magnetopause shape results from three sources of magnetic field. One source is the geomagnetic field produced by the Earth's dipole. The second results from an image dipole placed in front of the magnetopause to have the effect of the magnetopause current which limits the spatial extent of the geomagnetic field. The third is a southward IMF in the Earth's vicinity. To simplify the mathematical analysis, there is no plasma in the model. Moreover, the model does not include magnetic fields induced by the field-aligned current and the magnetotail current which are important elements of the magnetosphere.

We describe the geomagnetic field by

$$\boldsymbol{B_G} = B_E a^3 \frac{-3xz\hat{x} - 3yz\hat{y} + (x^2 + y^2 - 2z^2)\hat{z}}{(x^2 + y^2 + z^2)^{5/2}} \tag{1}$$

in terms of a southward magnetic dipole. Its magnetic moment is equal to the equatorial field strength B_E times the cube of the Earth's radius a. The magnetic field resulting from an image dipole is described by

$$\boldsymbol{B_P} = B_M a^3 \frac{-3(x - r_M)z\hat{x} - 3yz\hat{y} + ((x - r_M)^2 + y^2 - 2z^2)\hat{z}}{((x - r_M)^2 + y^2 + z^2)^{5/2}} \tag{2}$$

in terms of a southward dipole placed at $x = r_M$ on the x-axis. This image dipole in front of the magnetopause has a magnetic moment $B_M a^3$ greater than the geomagnetic moment. Namely, $B_M > B_E$ and $x_M > a$. The IMF is described by

$$\boldsymbol{B_I} = B_I \hat{z} \tag{3}$$

in terms of the strength of the IMF B_I, and its direction points southward for $B_I < 0$ and northward for $B_I > 0$. Here we use the Cartesian coordinates with the origin located at the Earth's center, the x-axis pointing toward the Sun, the y-axis toward the dusk, and the z-axis toward geomagnetic north. The total magnetic field is thus given by

$$\boldsymbol{B_G} + \boldsymbol{B_P} + \boldsymbol{B_I} = B_x\hat{x} + B_y\hat{y} + B_z\hat{z} \tag{4}$$

with

$$B_x = B_E a^3 \frac{-3xz}{(x^2+y^2+z^2)^{5/2}} + B_M a^3 \frac{-3(x-r_M)z}{((x-r_M)^2+y^2+z^2)^{5/2}} \tag{5}$$

$$B_y = B_E a^3 \frac{-3yz}{(x^2+y^2+z^2)^{5/2}} + B_M a^3 \frac{-3yz}{((x-r_M)^2+y^2+z^2)^{5/2}} \tag{6}$$

$$B_z = B_E a^3 \frac{x^2+y^2-2z^2}{(x^2+y^2+z^2)^{5/2}} + B_M a^3 \frac{(x-r_M)^2+y^2-2z^2}{((x-r_M)^2+y^2+z^2)^{5/2}} + B_I \tag{7}$$

Since regular field lines are smooth curves, these can provide a vivid visualization of the magnetopause shape. Regular field lines emanate from and terminate at neutral points at which the magnetic field strength becomes zero. The model magnetopause is a flux surface in which regular field lines emanate from and terminate at cusps corresponding to neutral points. Hence, the location of cusp neutral points plays a predominant role in the magnetopause shape. Before proceeding to draw magnetic field lines, it is essential to find out the location of cusp neutral points in the model.

In the model, neutral points occur where $\boldsymbol{B_G} + \boldsymbol{B_P}$ is canceled out by $\boldsymbol{B_I}$. For the $y = 0$ plane on which a cusp neutral point is located, by combining (5) and (7), the location of the cusp neutral point is determined by

$$\frac{B_M}{B_E} = \frac{x((x-r_M)^2+z^2)^{5/2}}{(r_M-x)(x^2+z^2)^{5/2}} \tag{8}$$

and

$$\frac{B_I}{B_E} = \frac{-r_M(r_M x - x^2 - 2z^2)a^3}{(r_M-x)(x^2+z^2)^{5/2}} \tag{9}$$

Since the model is assumed to be permeated by a southward IMF, the magnetopause shape appears symmetrical in both the $y = 0$ and $z = 0$ planes. Accordingly, the location of north and south cusp neutral points are symmetrical in the $z = 0$ plane. In this study, the distance from the Earth is normalized by the Earth's radius a and an image dipole strength is normalized by the magnetic field strength B_E at the the Earth's equator. However, B_I is converted to SI units by multiplying B_I/B_E by $B_E = 3.12 \times 10^4 nT$. Instead of directly solving (8) and

(9) for the location of cusp neutral points, we superimpose the contours of various B_M/B_E and B_I values with arbitrary r_M in the $x-z$ plane and find out the location of north and south cusp neutral points using the intersection of both contours. In situ measurements (e.g. Roelof and Sibeck, 1993) have shown that on average, the subsolar distance is $10a$. The subsolar distance is the standoff distance of the subsolar point where the solar wind dynamic pressure is balanced by the Earth's magnetic pressure. Hence, it is appropriate to choose a normalized r_M roughly twice the subsolar distance. For example, r_M is given as 20 (see Figure 1) and contours of various values of B_M/B_E and B_I are plotted over $4 \le x \le 9$ and $4 \le z \le 9$ in the meridian plane. Note that dotted lines denote B_M/B_E and solid lines B_I. With , r_M=20, B_M/B_E =8.6 and $B_I = -5nT$, Figure 1 shows that the north cusp neutral point is located at (x=5.7, z=6.2). This cusp location is consistent with satellite observations (cf. Frank, 1971). As a result, the location of cusp neutral points in the model is determined using r_M, B_M/B_E and B_I.

For given values of r_M, B_M/B_E and B_I, the flux surface of the magnetopause is constructed on the spatial extent of coplanar field lines leaving/entering north/south cusp neutral points. The integration of field lines is described by a differential equation as follows

$$\frac{dx}{B_x} = \frac{dy}{B_y} = \frac{dz}{B_z} = \frac{ds}{B} \tag{10}$$

where $(ds)^2 = (dx)^2 + (dy)^2 + (dz)^2$ and $B^2 = B_x^2 + B_y^2 + B_z^2$. Magnetic field lines in the neighborhood of a neutral point are determined by a linearized equation which can be derived from (10) with Taylor's expansion at the neutral point. Thus, the shape of the model magnetopause can be formed with footpoints at which coplanar field lines emanating from the south cusp neutral point are intercepted by the equatorial plane. The subsolar distance in the model is the location of one of the coplanar field lines emanating from the south cusp neutral point intercepted by the x-axis. Since the magnetic field strength reaches a minimum between the Earth's dipole and an image dipole, the subsolar distance in the model is limited by $x_M = r_M/(1+(B_M/B_E)^{1/4})$ where $\partial B_z/\partial x = 0$. The flank distance in the model is the location of one of the coplanar field lines emanating from the south cusp neutral point intercepted by the y-axis. As a result, the subsolar distance and the flank distance in the model are determined by a southward IMF, an image dipole strength and the location. In other words, the shape of the model magnetopause is determined by r_M, B_M/B_E and B_I.

3. THE MODEL MAGNETOPAUSE AND EMPIRICAL MODELS

As magnetohydrodynamic interaction of the terrestrial magnetosphere and flowing solar wind is in a state of equilibrium, the magnetopause current will be induced to shield the impinging solar wind. To balance the solar wind dynamic pressure D_p, the magnetic flux induced by the magnetopause current will enhance magnetic pressure at the dayside magnetopause. In the steady state, the magnetic pressure at the subsolar point is equal to D_p. In other words, the magnetic flux induced by the magnetopause current is proportional to D_p. With an

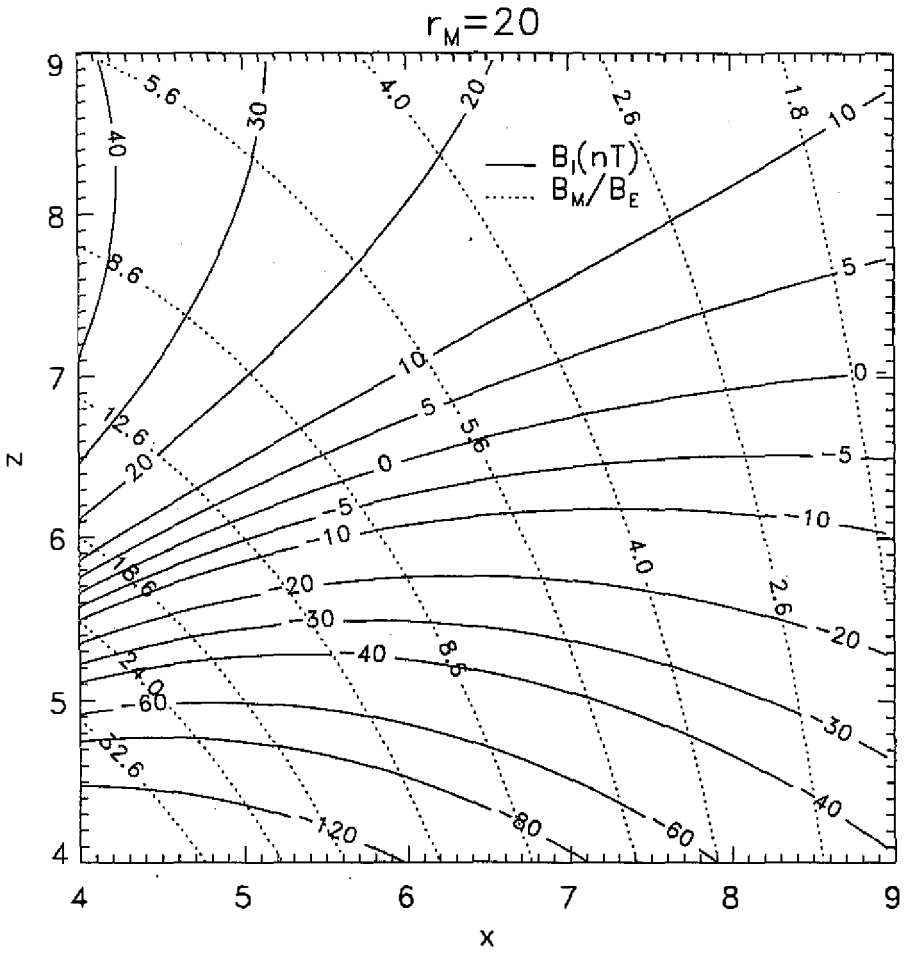

Fig. 1. An example of contours of various B_M/B_E and $B_I(nT)$ for r_M=20 superimposed in $x-z$ plane. Dotted lines denote B_M/B_E and solid lines B_I. Cusp neutral points can be located at the intersection of both contours of B_M/B_E and B_I.

image dipole and the location to produce the magnetic flux induced by the magnetopause current, the model magnetopause is an approximation of the dayside magnetopause. Hence, the shape of the model magnetopause can be regarded as being controlled by D_p and a southward IMF. In order to investigate how the magnetopause shape is controlled by the solar wind, we attempt to compare the shape of the model magnetopause with empirical models.

With an image dipole and the location to account for the effect of D_p, we first compare the shape of the model magnetopause with an empirical model by Roelof and Sibeck (1993). An ellipse of evolution was used by Roelof and Sibeck (1993) to fit the magnetopause shape, and they studied it by dividing magnetopause crossings into each bin of dynamic pressure D_p according to IMF B_z and IMF B_z according to D_p, respectively. Figure 9 of their cor-

rected version (Roelof and Sibeck, 1994) shows that the subsolar distance is about $8a - 12a$ and the flank distance is about $15a - 25a$ for various values of D_p and IMF B_z. In Figure 9 of Roelof and Sibeck (1994) there is a trend whereby for a constant IMF B_z, the magnetopause moves earthward in a similar shape with increasing pressure. In addition, their results show that the magnetopause around the subsolar point moves earthward and the flank expands with increasing IMF B_z for a constant dynamic pressure.

In the second section, we mentioned that the shape of the model magnetopause is determined by r_M, B_M/B_E and B_I. This means that the subsolar distance and the flank distance in the model are determined by r_M, B_M/B_E and B_I. For convenience of comparison with empirical results, we have to choose adequate values of r_M, B_M/B_E and B_I to calculate the shape of the model magnetopause. In the model, the subsolar distance is less than $x_M = r_M/(1+(B_M/B_E)^{1/4})$. Hence, the subsolar distance is determined by r_M and B_M/B_E. In Figure 2, it is shown that x_M varies as r_M and B_M/B_E change. In the five

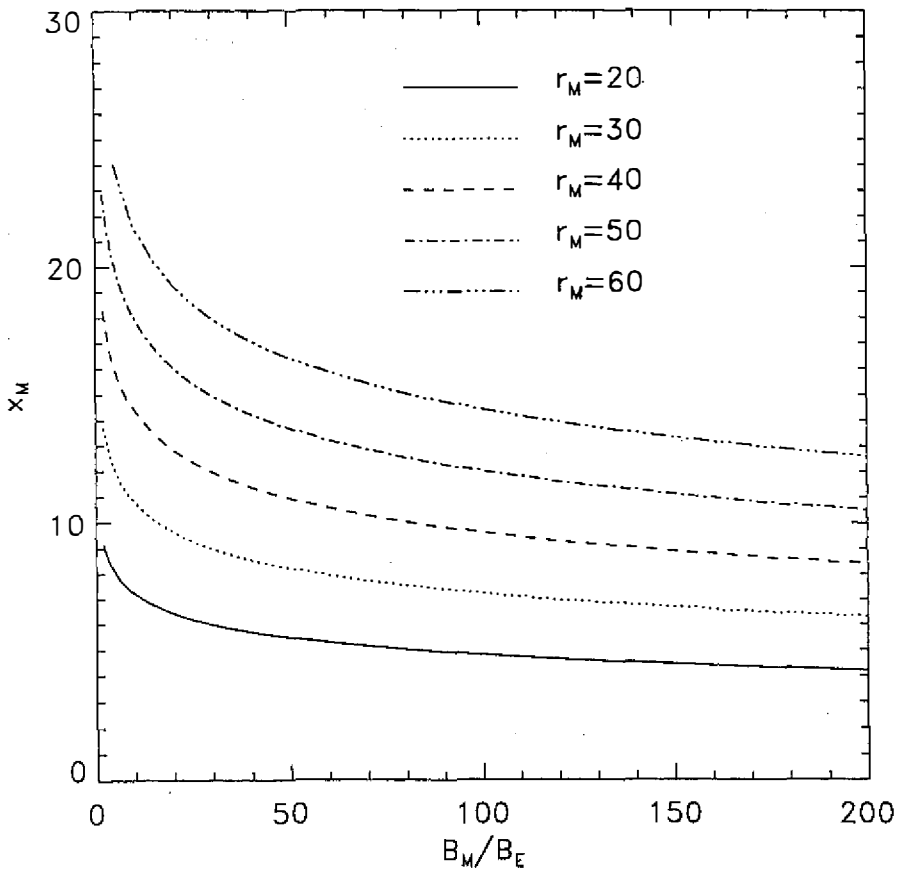

Fig. 2. A diagram of the relation between B_M/B_E and x_M for various r_M: r_M=20 (solid); r_M=30 (dotted); r_M=40 (dashed); r_M=50 (dashed-dotted); r_M=60 (dashed-dotted-dotted).

curves in Figure 2, the solid curve is for r_M=20, the dotted curve for r_M=30, the dashed curve for r_M=40, the dashed-dotted curve for r_M=50 and the dashed-dotted-dotted curve for r_M=60. Figure 2 shows that x_M is close to 10 when r_M has values of 30, 40, 50, 60 which correspond to B_M/B_E=14, 72, 190, 440, respectively. However, in Figure 3, it is shown that the flank distance shrinks as r_M and B_M/B_E increase. In contrast, the flank distance for r_M=30 and B_M/B_E=14 is consistent with the empirical fitting by Roelof and Sibeck (1994). By using this procedure, as shown in Figure 4, two curves are plotted for , r_M=30, $B_I = -2.5nT$ and values for B_M/B_E=14 and 14.5. To compare the observational result in the same unit, we

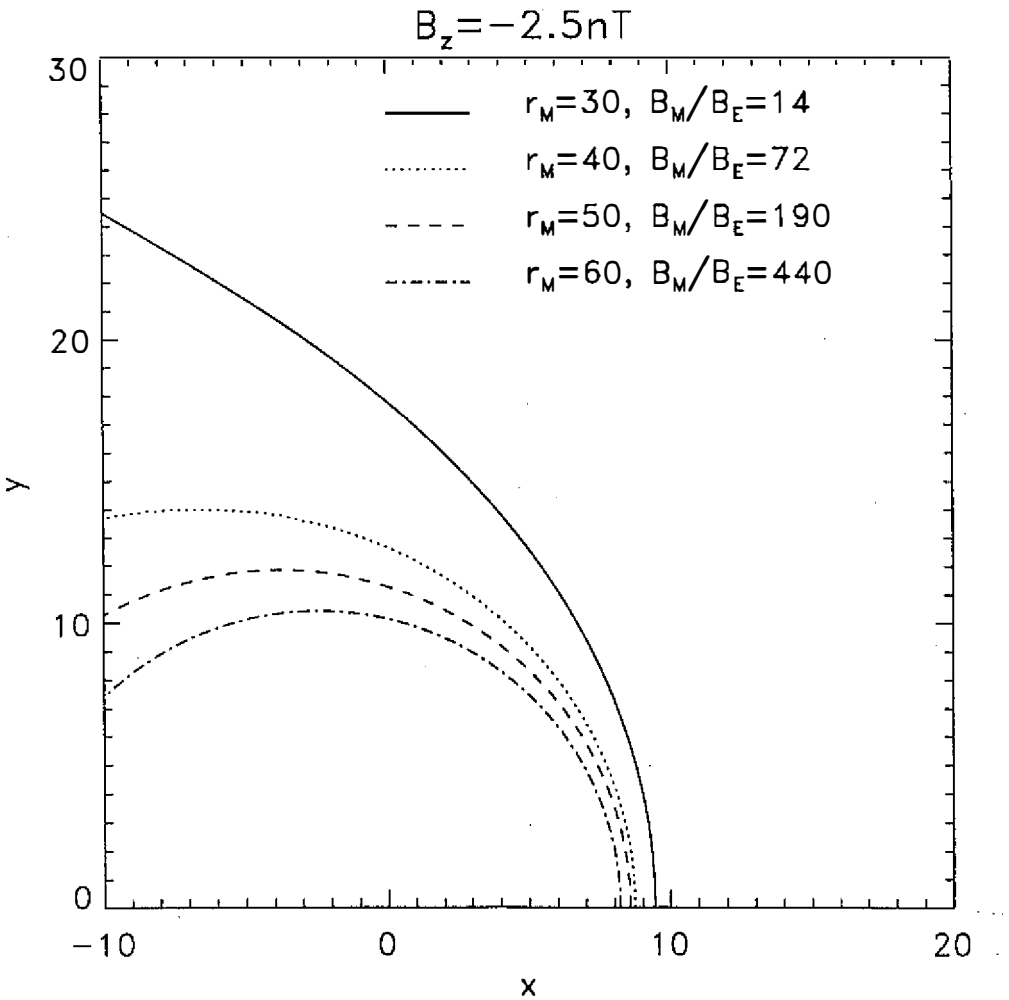

Fig. 3. The shape of the model magnetopause shape for $B_z = -2.5nT$ and various values of B_M/B_E and r_M : r_M=30 and B_M/B_E=14 (solid); r_M=40 and B_M/B_E=72 (dotted); r_M=50 and B_M/B_E=190 (dashed); r_M=60 and B_M/B_E=440 (dashed-dotted).

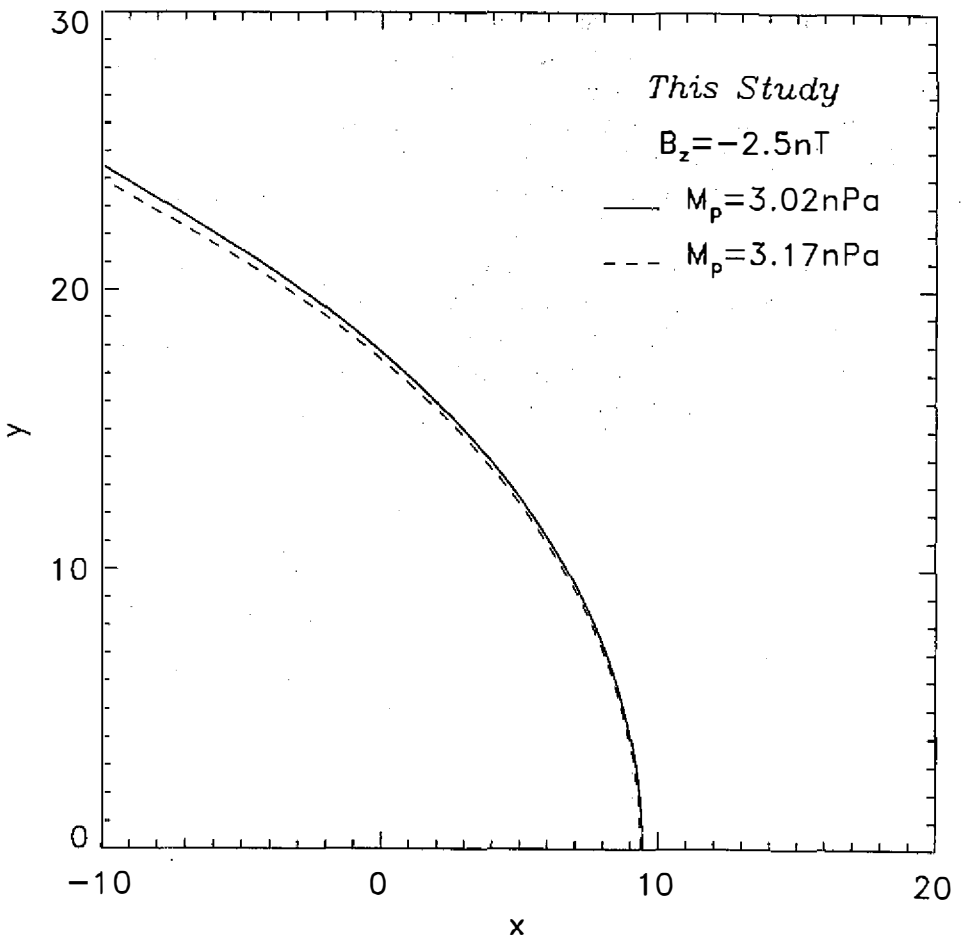

Fig. 4. The shape of the model magnetopause for r_M=30, $B_z = -2.5nT$ and various values of M_P: $M_P = 3.02nPa$ (solid); $M_P = 3.17nPa$ (dashed).

approximate D_p to the magnetic pressure at the subsolar point in the model and henceforth, B_I is rewritten as B_z. In the model, the magnetic pressure at the subsolar point is expressed as

$$M_P = \frac{B_{zs}^2}{2\mu_0} \tag{11}$$

where B_{zs} is the magnetic field at the subsolar point and μ_0 is the permeability in space. Thus, B_M/B_E=14 corresponds to $M_P = 3.02nPa$ and B_M/B_E=14.5 for $M_P = 3.17nPa$. In Figure 4, the solid curve is for $M_P = 3.02nPa$ and the dashed curve for $M_P = 3.17nPa$.

Note that the shape of the model magnetopause moves earthward in a similar way with increasing M_P for a constant B_z. It is evident from Figure 4 that there is a qualitative trend of dependence of the magnetopause shape upon the solar wind dynamic pressure for a constant B_z. The two curves in Figure 5 are for , r_M=30, $M_P = 3.3nPa$ (corresponding to B_M/B_E=15) and for B_z= −2.5 (dashed) and $-5.0nT$ (solid). In Figure 5, there is a trend of the flank expanding with increasing southward B_z for a constant D_p. However, the subsolar distance in Figure 5 seems constant for varying southward B_z. This is due to the subsolar distance in the model being limited by $x_M = r_M/(1+(B_M/B_E)^{1/4})$ which is independent of the southward B_z. Roelof and Sibeck(1993) also studied dependence of the subsolar distance upon D_p and southward B_z. They found that the subsolar distance varies less sensitively at high D_p for varying southward B_z. Hence, Figure 5 may be for high D_p and not for low D_p. By contrast, the shape of the model magnetopause is qualitatively consistent with the empirical fitting for a

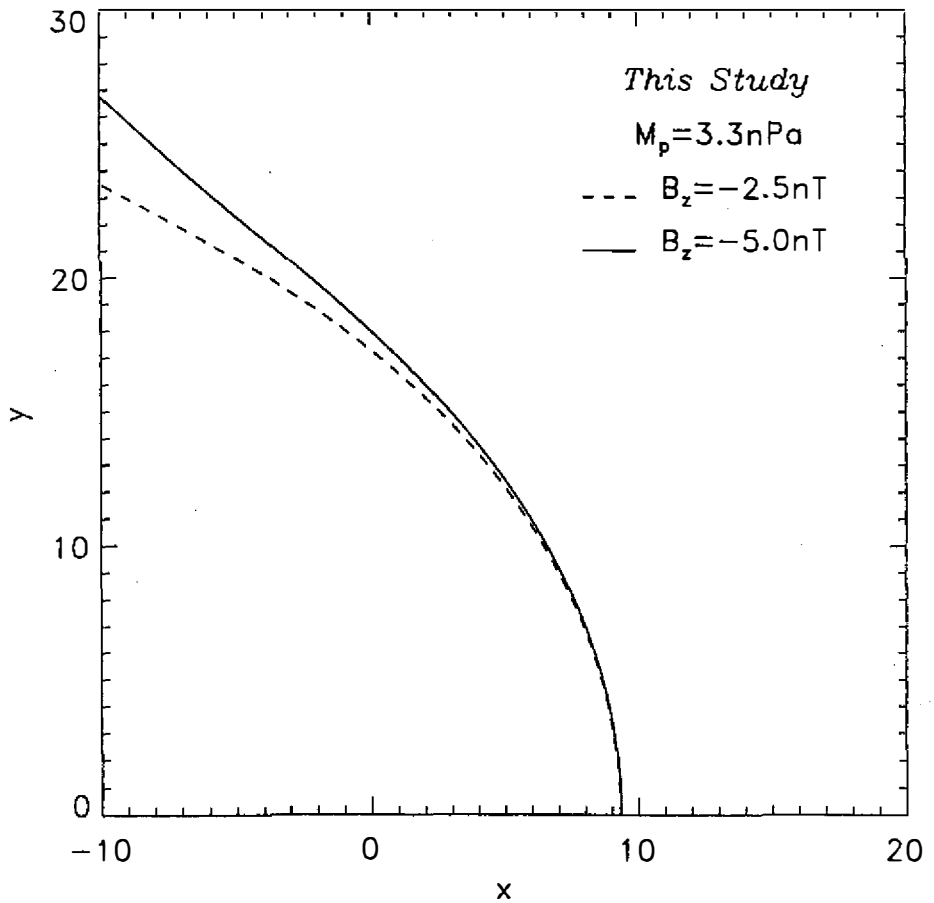

Fig. 5. The shape of the model magnetopause for r_M=30, $M_P = 3.3nPa$ and various values of the southward IMF: $B_z = -5.0nT$ (solid); $B_z = -2.5nT$ (dashed).

southward IMF. However, owing to a lack of variation of the subsolar distance in the model magnetopause, it is appropriate for high D_p only by comparison. Nevertheless, it implies that the magnetopause shape can be fitted as a function of the southward B_z, the image dipole strength and the location.

In order to verify whether an image dipole strength and the location can account for the effect of D_p, we investigate their relation with a comparison of the magnetopause shape fitted by a functional form proposed by Shue *et al.*(1997). According to Shue *et al.*(1997), the magnetopause shape can be fitted as

$$r = r_0(\frac{2}{1+\cos\theta})^{\alpha} \tag{12}$$

where r is the radial distance from the Earth's center to the magnetopause, r_0 is the distance from the Earth's center to the subsolar point and α is the exponential factor related to magnetopause flaring. For a southward IMF, the subsolar distance r_0 is derived as

$$r_0 = (11.2 + 0.14B_z)(D_P)^{-1/6.6} \tag{13}$$

and the flaring factor α is expressed as

$$\alpha = (0.58 - 0.01B_z)(1 + 0.01D_p) \tag{14}$$

From (13), D_p can be determined for given r_0 and a southward IMF B_z component. The subsolar distance in the model is the location of one of the coplanar field lines emanating from the south cusp neutral point intercepted by the x-axis. Hence, the subsolar distance r_0 can be acquired and substituted into (12) with a given B_z to get the corresponding value of D_p. In this study, the subsolar distance r_0 in the model is calculated with B_M/B_E varying from 14 to 16 for r_M=30 and the southward IMF B_z= -2.5 and $-5.0nT$. Figure 6 shows that M_P increases with increasing B_M/B_E. In Figure 6, the dotted line is for $B_z = -2.5nT$ and the solid line for $B_z = -5.0nT$. The relation between D_p and B_M/B_E is shown in Figure 7, with a dotted line for $B_z = -2.5nT$ and a solid line for $B_z = -5.0nT$. It is obvious from Figure 7 that D_p increases as B_M/B_E increases. Comparison of Figures 6 and 7 shows that for the southward IMF, the effect exerted by the solar wind dynamic pressure upon the dayside magnetopause can be approximated with an image dipole strength and the location.

To justify whether Figures 4 and 5 are for high D_p and the southward IMF, we reconstruct the magnetopause shape with the empirical model for the same parameters. By using (11), (12) and (13), the magnetopause shape based on the Shue *et al.*(1997) model is shown in Figures 8 and 9. Figure 8 shows the magnetopause shape for $B_z = -2.5nT$ with $D_p = 3.02nPa$ (solid) and $D_p = 3.17nPa$(dashed). The magnetopause shape in Figure 9 is for $D_p = 3.3nPa$ with the southward IMF values of $B_z = -2.5nT$(dashed) and $B_z = -5.0nT$

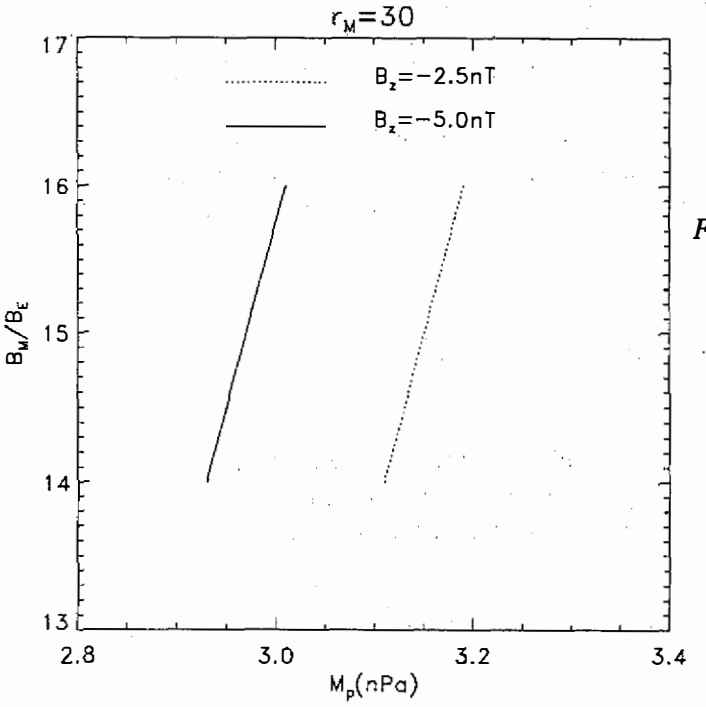

Fig. 6. A diagram of the relation between B_M/B_E and M_P for r_M=30 and various values of the southward IMF: $B_z = -5.0nT$ (solid); $B_z = -2.5nT$ (dotted).

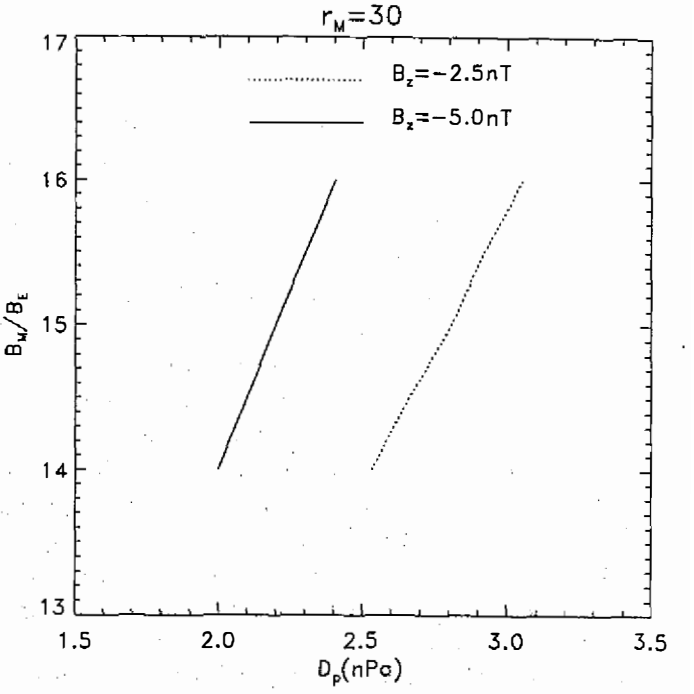

Fig. 7. A diagram of the relation between B_M/B_E and D_p for r_M=30 and various values of the southward IMF: $B_z = -5.0nT$ (solid); $B_z = -2.5nT$ (dotted).

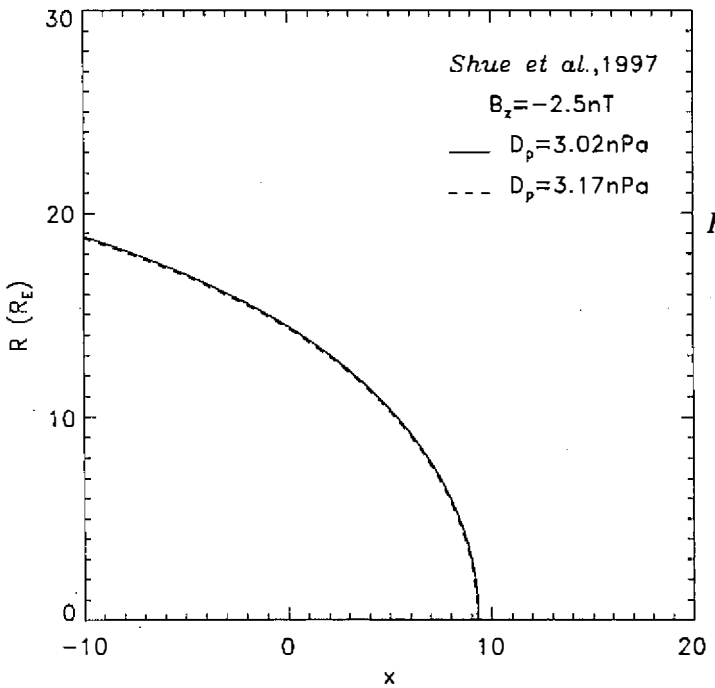

Fig. 8. The magnetopause shape for a southward IMF $B_z = -2.5nT$ and various values of dynamic pressures reproduced from the Shue *et al.*(1997) model: $D_p = 3.02nPa$ (solid); $D_p = 3.17nPa$ (dashed).

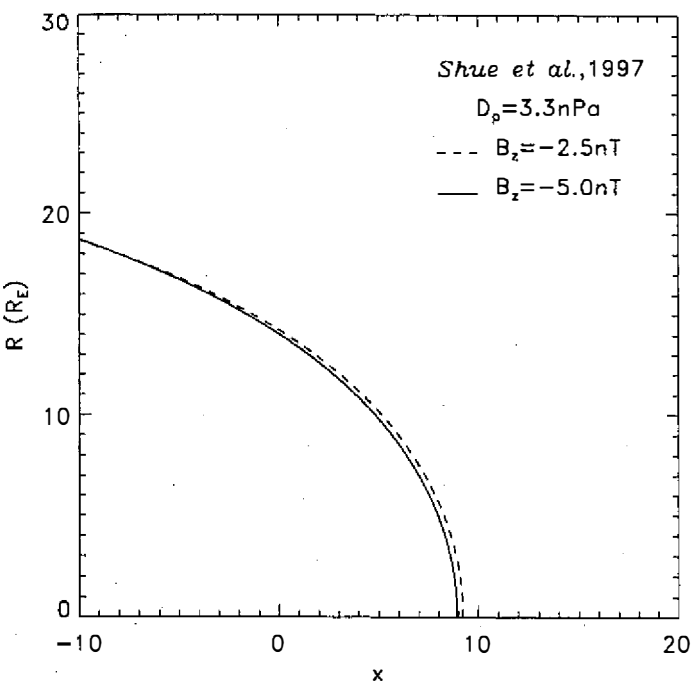

Fig. 9. The magnetopause shape for $D_p = 3.3nPa$ and various values of the southward IMF reproduced from the Shue *et al.*(1997) model: $B_z = -5.0nT$ (solid); $B_z = -2.5nT$ (dashed).

(solid). In contrast, for the dayside region, both models of the magnetopause shape are consistent with each other except for the flank distance. Hence, we justify that Figures 4 and 5 are for high D_p and a southward IMF.

4. DICUSSION AND SUMMARY

In this study, the shape of the model magnetopause is obtained in the equatorial plane. Since the dayside magnetospause is axis-symmetric, the shape of the model magnetopause can be regarded as an approximation of the magnetopause shape observed by satellites in low-latitude orbits. For the same subsolar distance and the same flank distance, M_P in Figures 4 and 5 seems larger than D_p in the empirical fitting by Roelof and Sibeck (1994). This implies that the geomagnetic field at the subsolar point may be overestimated with the Earth's dipole and given image dipole. On the other hand, there is a view that the reduction of the subsolar distance may result from the flux erosion due to the subsolar reconnection (e.g. Paschman *et al.*, 1986). In this study, the model magnetosphere is based on a mathematical model by Yeh (1997) which is characterized by a pair of cusp neutral points in the noon meridian and a segmental neutral line on the equatorial plane. In a steady state, magnetic reconnection in this model magnetosphere occurs at the flank with the exception of at the subsolar point. Hence, this model magnetosphere may not explain the flux erosion in the subsolar region. In Figure 5, there is also a trend whereby increased B_z enhances tail flaring as D_p corresponding to M_P remains constant. This result is consistent with the prediction by Petrinec and Russell (1993) that tail flaring is associated with a southward IMF B_z. It is worth noting that the flank distance in Figures 4 and 5 are inconsistent with Figures 8 and 9. This discrepancy shows that the dipole's strength B_M/B_E in the theoretical model may not account for the total effect of the solar wind. Nevertheless, the model provides a preliminary theoretical explanation on how the magnetopause shape is controlled by the solar wind.

Instead of solving the location of a cusp neutral point analytically, we have presented an alternative approach to finding the location by using the intersection of both contours of B_M/B_E and B_I for a specific r_M in the meridian plane. By using the integration of coplanar field lines emanating from a south cusp neutral point, we have constructed the shape of the model magnetopause which consists of the footpoints of coplanar field lines in the equatorial plane. With an image dipole strength and the location to account for the effect of the solar wind dynamic pressure, the shape of the model magnetopause is compared to the empirical model by Roelof and Sibeck (1993) for a southward IMF. With B_M/B_E ~14 and r_M=30, the shape of the model magnetopause is consistent with the empirical fitting by Roelof and Sibeck (1994) for a southward IMF. The comparison shows that in both models the dayside magnetopause moves earthward with increased dynamic pressure for a constant southward IMF. Moreover, the flank in both models expands as the southward IMF increases for a constant D_p. The relation between the image dipole strength at a fixed location and D_p is examined by using a functional form by Shue *et al.*(1997), and it shows that they are linearly correlated. Hence, it is verified that the effect exerted by the solar wind dynamic pressure can be approximated by an image dipole strength and the location. With the exception of the flank distance, for high D_p and southward IMF, the magnetopause shape based on Shue *et al.*(1997) is consistent with our results.

In summary, this study provides a qualitative description on the solar wind control of the magnetopause shape and it shows that the magnetopause shape can be fitted as a function of the southward IMF, the image dipole strength and the location. In addition, the shape of the model magnetopause is consistent with empirical models for high D_p with a southward IMF.

Acknowledgments The author thanks Prof. J. K. Chao of National Central Unversity for useful suggestions and comments to improve this work. This work was supported by the National Science Council of R.O.C. in Taiwan under grant NSC87-2111-M-008-AP8.

REFERENCES

Chapman, S., and V. C. A. Ferraro, 1931: A new theory of magnetic storms. *J. Geophys. Res.*, **36**, 171-186.

Dungey, J. W., 1961: Interplanetary magnetic field and the auroral zones. *Phy. Rev. Lett.*, **6**, 47-48.

Fairfield, D. H., 1987: Structure of the geomagnetic tail, In Magnetotail Physics. In: A. T. Y. Lui (Ed.), Johns Hopkins University Press, Baltimore, Md., 23-33 pp.

Fairfield, D. H., 1995: Observations of the shape and location of the magnetopause: a review, in Physics of the Magnetopause. In: P. Song, B.U.O. Sonnerup and M. F. Thomsen (Eds.), American Geophysical Union, 53-60 pp.

Frank, L. A., 1971: Plasma in Earth's polar magnetosphere. *J. Geophys. Res.*, **76**, 5202-5219.

Haerendel, G., G. Paschmann, N. Sckopke, H. Rosenbauer, and P. C. Hedgecock, 1978: The front side boundary layer of the magnetopause and the problem of reconnection. *J. Geophys. Res.*, **83**, 3195-3216.

Nishida, A., 1978: Geomagnetic diagnosis of the magnetosphere, Springer-Verlag, Berlin, 1-12 pp.

Paschmann, G., I. Papamastorakis, W. Baumjohann, N. Sckopke, C. W. Carlson, B. U. O. Sonnerup, and H. Luhr, 1986: The magnetopause for large magnetic shear: AMPTE/IRM observations. *J. Geophys. Res.*, **91**, 11099-11115.

Petrinec, S. P., and C. T. Russell, 1993: An empirical model of the size and shape of the near-Earth magnetotail. *Geophys. Res. Lett.*, **20**, 2695-2698.

Petrinec, S. P., P. Song and C. T. Russell, 1991: Solar cycle variations in the size and shape of the magnetopause. *J. Geophys. Res.*, **96**, 7893-7896.

Roelof, E. C., and D. G. Sibeck, 1993: Magnetopause shape as a bivariate function of interplanetary magnetic field and solar wind dynamic pressure. *J. Geophys. Res.*, **98**, 21421-21450.

Roelof, E. C., and D. G. Sibeck, 1994: Correction to "Magnetopause shape as a bivariate function of interplanetary magnetic field and solar wind dynamic pressure" by Edmond C. Roelof and David G. Sibeck. *J. Geophys. Res.*, **99**, 8787-8789.

Shue, J. H., J. K. Chao, H. C. Fu, C. T. Russell, P. Song, K. K. Khurana and H. J. Singer, 1997: A new functional form to study the solar wind control of the magnetopause size and shape. *J. Geophys. Res.*, **102**, 9497-9511.

Sibeck, D. G., R.E. Lopez, and E.C. Roelof, 1991: Solar wind control of the magnetopause

shape, location, and motion. *J. Geophys. Res.*, **96**, 5489-5495.

Yeh, T., 1997: Magnetospheric structure with a southward interplanetary magnetic field. *J. Geophys. Res.*, **102**, 51-56.